Check for updates

Exactly solvable 1D model explains the low-energy vibrational level structure of protonated methane†

Jonathan I. Rawlinson, [ID] *[a] Csaba Fábri [ID] [bc] and Attila G. Császár [ID] [bc]

A new one-dimensional model is proposed for the low-energy vibrational quantum dynamics of CH_5^+ based on the motion of an effective particle confined to a 60-vertex graph Γ_{60} with a single edge length parameter. Within this model, the quantum states of CH_5^+ are obtained in analytic form and are related to combinatorial properties of Γ_{60}. The bipartite structure of Γ_{60} gives a simple explanation for curious symmetries observed in numerically exact variational calculations on CH_5^+.

Protonated methane, CH_5^+, also called methonium, is considered to be the prototype of pentacoordinated nonclassical carbonium ions.[1–3] The curious carbonium cations yielded an extremely rich chemistry and a Nobel prize to their discoverer, George Olah.[4] Nevertheless, these are not the only sources of fame for carbonium ions and in particular for CH_5^+. Over the last two decades,[5] the internal motion of CH_5^+ has been posing a formidable challenge to high-resolution spectroscopists.[5–15] The most outstanding issue is that the observed spectra of CH_5^+ remain exceptionally complex even when they are observed at temperatures of a few K,[9,13] due to the quasistructural nature[16] of this molecular ion.

As to the utilization of quantum chemistry to solve the experimental puzzle, through huge numerical efforts accurate rovibrational energy levels and eigenstates have been made available for CH_5^+ in recent years.[7,12,14] These studies have revealed close-lying clusters in the rovibrational energy levels, with fascinating symmetry characteristics. These features have defied explanation by conventional means, motivating the development of novel models for CH_5^+. The most important models put forward so far are as follows: (a) particle-on-a-sphere (POS),[17–23] (b) five-dimensional (5D) rotor (superrotor),[24–26] and (c) quantum graph.[15,27] So far, the quantum-graph model seems to have resulted in the most satisfactory explanation of the low-energy quantum dynamics of CH_5^+, including both vibrations[15] and rotations.[27]

Quantum graphs have a long history in chemistry and physics, dating back to Linus Pauling's description of electrons in organic molecules in the 1930s.[28] They have only recently been introduced to the study of nuclear dynamics, where they have proved useful in high-resolution spectroscopy[15,27] and also in explaining α-cluster dynamics in nuclear physics.[29,30] Quantum graphs[31] are metric graphs, that is each of their edges possesses a length. In the context of rovibrational dynamics of molecules, each vertex of the graph represents a version[32] of an equilibrium structure. Depending on the nuclear permutation-inversion symmetry[32] of the molecule of a given composition, even if the molecule has a single minimum on a given potential energy surface it may possess a large number of versions. The vertices defined by the versions are connected by edges which represent collective internal motions converting different versions into each other. Once a quantum graph is set up, one constructs the one-dimensional (1D) Schrödinger equation for an effective particle confined to the graph and solves it to determine the energy levels and eigenstates (ESI†). In this way, the complex multidimensional rovibrational quantum dynamics of a polyatomic molecule is mapped onto the effective motion of a 1D particle confined to a much simpler space.

In the case of CH_5^+, the equilibrium structure, the only one found on its ground electronic state, is composed of a H_2 unit sitting on top of a CH_3^+ tripod, an arrangement with C_s point-group symmetry. The five protons can be rearranged in 5! = 120 ways, generating 120 symmetry-equivalent versions. These versions become the 120 vertices of a quantum graph Γ_{120}.[15] There are two types of motion interconverting the 120 versions, equivalent to scrambling the H atoms of CH_5^+: the internal rotation of the H_2 unit by 60° (both clockwise and counterclockwise), and the flip motion that exchanges a pair of protons between the H_2 and CH_3^+ units. The barriers to these motions on the potential energy hypersurface of CH_5^+[33] are known to be

a School of Mathematics, University of Bristol, Bristol, UK.
E-mail: jonathanianrawlinson@gmail.com

b Laboratory of Molecular Structure and Dynamics, Institute of Chemistry,
ELTE Eötvös Loránd University, Pázmány Péter sétány 1/A,
Budapest H-1117, Hungary

c MTA-ELTE Complex Chemical Systems Research Group, P.O. Box 32,
Budapest 112 H-1518, Hungary

Table 1 The block structure characterizing the first 60 vibrational states of CH_5^+, revealed in variational nuclear-motion computations.[12,14] The numbers in parentheses give the total number of positive and negative parity states within a block

Block 1	Block 2
0–60 cm^{-1} (15,15)	110–200 cm^{-1} (15,15)
$A_1^+ \oplus G_1^+ \oplus H_1^+ \oplus H_2^+ \oplus$	$G_1^+ \oplus H_1^+ \oplus I^+ \oplus$
$G_2^- \oplus H_2^- \oplus I^-$	$A_2^- \oplus G_2^- \oplus H_1^- \oplus H_2^-$

relatively low. It is plausible that the low-energy dynamics is dominated by motion along these particular paths, so that motions other than the internal rotation and flip motions can be disregarded. Thus, one can take these motions to correspond to the edges of Γ_{120}. As one flip edge and two internal rotation edges are connected to each vertex of Γ_{120}, each vertex has a degree of three (Γ_{120} is a 3-regular graph). Due to the nature of the underlying internal motions, the 120 internal rotation and 60 flip edges are assigned effective lengths L_{rot} and L_{flip}, respectively.

As shown before,[15,27] the quantum graph Γ_{120} reproduces the low-energy rovibrational energy levels of CH_5^+, as well as of CD_5^+, remarkably well when optimized values are used for L_{flip} and L_{rot} (ESI†). For instance, the Γ_{120} model perfectly reproduces the curious block structure (states occuring in groups of 15 and 30, see Table 1) of the vibrational eigenstates of CH_5^+, first noted in a variational study of Wang and Carrington[12] and later confirmed in ref. 14. As seen in Table 1, rovibrational eigenstates of CH_5^+ are labelled by irreducible representations (irreps) of the molecular symmetry (MS) group[32] $S_5^* = S_5 \times \{E,E^*\}$, generated by S_5 permutations of the five protons together with spatial inversion E^* (E denotes the identity operation).

Beyond the existence of blocks, in Table 1 one can notice other clear symmetry relations for the first 60 quantum states. A comparison of the group-theoretic relation

$$\left(A_1^+ \oplus G_1^+ \oplus H_1^+ \oplus H_2^+\right) \otimes A_2^- \simeq A_2^- \oplus G_2^- \oplus H_2^- \oplus H_1^- \quad (1)$$

with the data in Table 1 suggests a direct correspondence between the 15 positive-parity states in Block 1 [appearing on the left-hand side (LHS) of eqn (1)] and the 15 negative-parity states in Block 2 [right-hand side (RHS) of eqn (1)]. Likewise,

$$\left(G_2^- \oplus H_2^- \oplus I^-\right) \otimes A_2^- \simeq G_1^+ \oplus H_1^+ \oplus I^+, \quad (2)$$

suggesting a link between the 15 negative-parity states in Block 1 and the positive-parity states in Block 2. These remarkable symmetry relations have been lacking any simple explanation, even in terms of the Γ_{120} model. As this paper proves, introduction of the simplest quantum-graph model, Γ_{60}, of the quantum dynamics of CH_5^+, derived from Γ_{120}, is sufficient to explain the curious energy-level and symmetry structure of the lowest vibrational states of CH_5^+, and, as a bonus feature, it allows the analytic determination of the quantum states of the model problem.

Let us start our journey toward the simplest model with the quantum graph Γ_{120}. We recall two important characteristics of our original study.[15] First, we neglect the potential energy along the edges of Γ_{120}, since the barriers to the internal rotation and flip motions are small (about 30 cm^{-1} and 300 cm^{-1}, respectively[33]). Second, we fix the effective edge lengths L_{flip} and L_{rot}. In ref. 15 this was done by an optimization procedure to give the best fit to either 7D or 12D reference data. In both cases the optimized L_{flip} was much smaller than the optimized L_{rot}, with the ratio $L_{flip}/L_{rot} = 1.0/61.2$ in the 7D case.

Our new model is based on the following idea: the ratio L_{flip}/L_{rot} is so small that it is tempting to imagine shrinking the flip edges to zero length, identifying the two vertices at the endpoints of each flip edge to give a single vertex. Setting $L_{flip} = 0$ has a negligible effect on the accuracy of the fit, at least at low energies. At the same time, this approximation gives a huge simplification: the number of vertices is halved and we get a new quantum graph, Γ_{60}, with only the internal rotation edges remaining. It is reasonable to identify each new vertex with the midpoint of the (now contracted) flip edge, which is a C_{2v}-symmetric transition state, as illustrated in Fig. 1. Γ_{60} represents 60 symmetry-equivalent versions of this configuration. We propose that the most important characteristics of the low-energy vibrational quantum states of CH_5^+ can be understood in terms of a 1D, potential-free motion between these versions corresponding to the vertices of the quantum graph Γ_{60}. Note that each vertex is connected to precisely four other vertices, as shown also in Fig. 1, giving rise to the 4-regular (quartic) quantum graph Γ_{60}, illustrated in Fig. 2.

There is an alternative way of rationalizing the above contraction procedure. At the energies we are interested in, one can show that the Γ_{120} wave functions for the energy eigenstates are approximately constant along the flip edges. In this limit, the boundary conditions of Γ_{120} become equivalent to those of Γ_{60} (ESI†). Either way, Γ_{60} only retains edges corresponding to the internal rotation. Our simplified model therefore has the feature of explaining the low-energy dynamics solely in terms
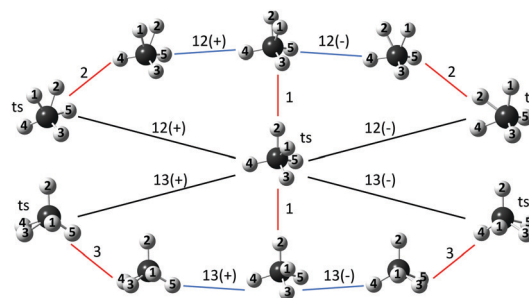

Fig. 1 Local structure of the quantum graphs Γ_{120} (blue and red edges) and Γ_{60} (black edges). The red edges correspond to the flip motion and the labels indicate which proton is exchanged from a H_2 unit to a CH_3^+ unit. The blue edges correspond to an internal rotation and the labels indicate the H_2 unit which rotates relative to the CH_3^+ unit in a clockwise (+) or anticlockwise (−) fashion. The midpoint of each red flip edge is a C_{2v}-symmetric transition state (ts). In going from Γ_{120} to Γ_{60}, the red edges shrink so that we are left with just the transition states connected by black edges.
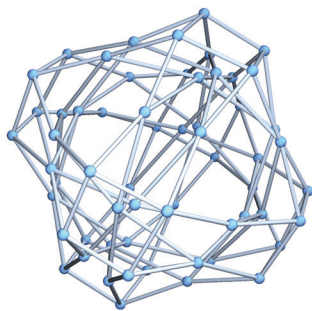
Fig. 2   Illustration of the 4-regular quantum graph Γ_{60}. In this model of the quantum dynamics of CH_5^+ there is a single edge length, connecting versions of C_{2v}-symmetric transition states, corresponding to midpoints of the flip edge of Γ_{120}.

of the internal rotation motion without the flip motion, with the constant wave function argument allowing for backstage full exchange of the protons. This model is thus set up in clear violation of the claim of the authors of ref. 34, namely that "the combination of the two [internal motions] enables large-amplitude motion and thus full scrambling ... whereas partial scrambling leads to the well-known small-amplitude motion only".

We now seek the quantum states corresponding to motion on the Γ_{60} graph. The eigenenergies are found by solving the time-independent Schrödinger equation for a freeeffective particle moving along the edges, with the so-called Neumann boundary conditions[31] imposed on the eigenstates. These conditions are that the wave function should be continuous everywhere, with zero total momentum flux out of each vertex. As we have already pointed out, Γ_{60} is a 4-regular graph with all edges having a common length $l = L_{rot}$. Perhaps surprisingly, these properties imply that the structure of the quantum energy levels can be determined entirely from combinatorial properties of the graph.

More precisely, given a wave function ψ defined on the graph Γ_{60} and obeying the time-independent Schrödinger equation along each edge,

$$-\frac{1}{2}\frac{d^2\psi}{dx^2} = E\psi, \tag{3}$$

where x is a mass-scaled coordinate, consider the vector of its values at each vertex $\mathbf{v} = (\psi(v_1), \psi(v_2), \ldots)$. It is straightforward to prove (ESI†) that ψ is an eigenfunction with energy E satisfying the Neumann boundary conditions if and only if

$$\mathbf{A}\mathbf{v} = 4\cos\left(\sqrt{2E}l\right)\mathbf{v}, \tag{4}$$

i.e., if and only if $\lambda = 4\cos(\sqrt{2E}l)$ is an eigenvalue of the adjacency matrix $\mathbf{A}$ for the graph Γ_{60}, with $\mathbf{v}$ in the corresponding eigenspace. $\mathbf{A}$ is simply a matrix whose elements indicate whether given pairs of vertices are connected by an edge or not:

$$(\mathbf{A})_{ij} = \begin{cases} 1 & \text{if vertices } v_i \text{ and } v_j \text{ connected} \\ 0 & \text{otherwise} \end{cases} \tag{5}$$

and is a familiar concept in elementary graph theory.[35]

Eqn (4) therefore relates the *quantum spectrum* (the eigenvalues of the Hamiltonian) to the so-called *combinatorial spectrum* (the eigenvalues of the adjacency matrix). The combinatorial spectrum is a concept already utilized in molecular spectroscopy,[36] and only depends on the connectivity of the graph as encoded in $\mathbf{A}$.

To find the combinatorial spectrum of Γ_{60}, we look for roots of the characteristic polynomial $\chi_{\mathbf{A}}(\lambda) = \det(\lambda\mathbf{I} - \mathbf{A})$ associated with the adjacency matrix $\mathbf{A}$. An explicit expression for $\mathbf{A}$ is easily derived by considering paths of the form illustrated in Fig. 1. In the end, we obtain

$$\chi_{\mathbf{A}}(\lambda) = (\lambda^4 - 9\lambda^2 + 16)^5(\lambda^4 - 12\lambda^2 + 16)^4(\lambda^2 - 1)^{11}(\lambda^2 - 16), \tag{6}$$

and the full combinatorial spectrum is given in Table 2. Table 2 also shows the dimensions of the corresponding eigenspaces and the irreps of the MS group $S_5^\star$.

We pause here to note the striking similarity between Tables 1 and 2. First, note that the combinatorial spectrum splits into positive λ and negative λ, with each corresponding to a total eigenspace dimension of 30. Moreover, the eigenspaces associated with positive λ transform in precisely the same irreps as Block 1 of Table 1, while those associated with negative λ transform precisely like Block 2. Thus, purely combinatorial properties of the quantum graph Γ_{60} have captured the block structure of the lowest vibrational states of CH_5^+. Even more interestingly, we have an explanation for the curious relationship between Block 1 states and Block 2 states: this corresponds to a $\lambda \to -\lambda$ symmetry of the combinatorial spectrum (see Table 2), under which the $S_5^\star$ irreps are related by multiplication with A_2^-. The symmetry of the combinatorial spectrum under $\lambda \to -\lambda$ is a simple consequence[35] of the fact that the quantum graph Γ_{60} is *bipartite*: the set of vertices V can be divided into two disjoint and independent sets A and B such that every edge connects a vertex in A to one in B. The sets A and B are related by odd permutations of the protons (ESI†).

Table 2   The combinatorial spectrum of the quantum graph Γ_{60}, where dim (λ) gives the degeneracy of a given eigenvector corresponding to the eigenvalue λ [see eqn (6)]

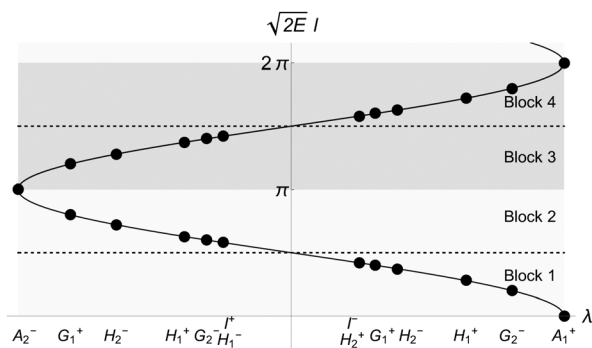| λ	dim(λ)	$S_5^\star$ irrep
4	1	A_1^+
$1 + \sqrt{5}$	4	G_2^-
$\frac{1}{2}(1 + \sqrt{17})$	5	H_1^+
$\frac{1}{2}(-1 + \sqrt{17})$	5	H_2^-
$-1 + \sqrt{5}$	4	G_1^+
1	11	$H_2^+ \oplus \Gamma^-$
-1	11	$H_1^- \oplus I^+$
$1 - \sqrt{5}$	4	G_2^-
$\frac{1}{2}(1 - \sqrt{17})$	5	H_1^+
$\frac{1}{2}(-1 - \sqrt{17})$	5	H_2^-
$-1 - \sqrt{5}$	4	G_1^+
-4	1	A_2^-

Fig. 3 Illustration of the block structure and the symmetry properties of the spectrum of the quantum graph Γ_{60}. Black dots indicate energies of the quantum states.

Eqn (4) relates the combinatorial spectrum to the quantum spectrum, as illustrated in Fig. 3. We can see the consequences of the $\lambda \to -\lambda$ symmetry for the quantum energy levels: each state in Block 1 comes with a partner in Block 2, with their corresponding values of $\sqrt{2El}$ being related by reflection in the line $\sqrt{2El} = \pi/2$. In particular, the dimensionless ratios

$$\frac{\sqrt{E_1(I^-)} + \sqrt{E_2(I^+)}}{\sqrt{E_1(H_1^+)} + \sqrt{E_2(H_2^-)}}, \frac{\sqrt{E_1(H_2^+)} + \sqrt{E_2(H_1^-)}}{\sqrt{E_1(H_1^+)} + \sqrt{E_2(H_2^-)}}, \ldots \quad (7)$$

are all equal to 1 in the Γ_{60} model. These dimensionless ratios agree with the variational seven-dimensional model[7,12,14] results to within 20 percent (see the ESI†).

In this paper we have drastically simplified the quantum graph model of the low-energy rovibrational quantum dynamics of CH_5^+ by reducing the original 120-vertex quantum graph to a 60-vertex graph, Γ_{60}. Γ_{60} was constructed by shrinking the edges corresponding to the flip internal motion that exchanges a pair of protons between the H_2 and CH_3^+ units of the equilibrium structure of CH_5^+. Thus, at first sight we neglect one of the two important large-amplitude internal motions characterizing the exchange dynamics (scrambling) of the H atoms of CH_5^+. This allows us to obtain the quantum states of Γ_{60} in analytic form, with the structure of the energy levels depending only on combinatorial properties. The eigenvalues of this simple 1D, potential-free model are in excellent agreement with the energies of the first 60 vibrational states determined by sophisticated variational nuclear-motion computations utilizing a potential energy hypersurface. Furthermore, the bipartite structure of Γ_{60} gives a natural explanation for symmetries in the vibrational energy-level structure of CH_5^+, again in perfect agreement with the results of variational nuclear-dynamics computations. Note that neither the variational computations[7,12,14] nor the quantum-graph models[15,27] yield only the Pauli-allowed states of CH_5^+ (states with $A_2^\pm$, $G_2^\pm$, and $H_2^\pm$ symmetry have non-zero spin-statistical weights), so our discussion focused on *all* possible states; the non-existing states can be filtered out *a posteriori*.

Conflicts of interest

There are no conflicts to declare.

Notes and references

1 G. A. Olah and R. H. Schlosberg, *J. Am. Chem. Soc.*, 1968, **90**, 2726–2727.
2 G. A. Olah, G. Klopman and R. H. Schlosberg, *J. Am. Chem. Soc.*, 1969, **91**, 3261–3268.
3 G. A. Olah, *Carbocations and Electrophilic Reactions*, VCH-Wiley Publishers, Weinheim, 1974.
4 G. A. Olah, *My Search for Carbocations and Their Role in Chemistry*, 1994, pp. 149–176.
5 E. T. White, J. Tang and T. Oka, *Science*, 1999, **284**, 135–137.
6 O. Asvany, P. Padma Kumar, B. Redlich, I. Hegemann, S. Schlemmer and D. Marx, *Science*, 2005, **309**, 1219–1222.
7 X.-G. Wang and T. Carrington Jr., *J. Chem. Phys.*, 2008, **129**, 234102.
8 S. D. Ivanov, O. Asvany, A. Witt, E. Hugo, G. Mathias, B. Redlich, D. Marx and S. Schlemmer, *Nat. Chem.*, 2010, **2**, 298–302.
9 O. Asvany, K. M. T. Yamada, S. Brünken, A. Potapov and S. Schlemmer, *Science*, 2015, **347**, 1346–1349.
10 R. Wodraszka and U. Manthe, *J. Phys. Chem. Lett.*, 2015, **6**, 4229–4232.
11 H. Schmiedt, S. Schlemmer and P. Jensen, *J. Chem. Phys.*, 2015, **143**, 154302.
12 X.-G. Wang and T. Carrington, *J. Chem. Phys.*, 2016, **144**, 204304.
13 S. Brackertz, S. Schlemmer and O. Asvany, *J. Mol. Spectrosc.*, 2017, **342**, 73–82.
14 C. Fábri, M. Quack and A. G. Császár, *J. Chem. Phys.*, 2017, **147**, 134101.
15 C. Fábri and A. G. Császár, *Phys. Chem. Chem. Phys.*, 2018, **20**, 16913–16917.
16 A. G. Császár, C. Fábri and J. Sarka, *Wiley Interdiscip. Rev.: Comput. Mol. Sci.*, 2020, **10**, e1432.
17 G. A. Natanson, G. S. Ezra, G. Delgado-Barrio and R. S. Berry, *J. Chem. Phys.*, 1984, **81**, 3400–3406.
18 G. A. Natanson, G. S. Ezra, G. Delgado-Barrio and R. S. Berry, *J. Chem. Phys.*, 1986, **84**, 2035–2044.
19 D. M. Leitner, G. A. Natanson, R. Berry, P. Villarreal and G. Delgado-Barrio, *Comput. Phys. Commun.*, 1988, **51**, 207–216.
20 J. E. Hunter, D. M. Leitner, G. A. Natanson and R. Berry, *Chem. Phys. Lett.*, 1988, **144**, 145–148.
21 M. P. Deskevich and D. J. Nesbitt, *J. Chem. Phys.*, 2005, **123**, 084304.
22 M. P. Deskevich, A. B. McCoy, J. M. Hutson and D. J. Nesbitt, *J. Chem. Phys.*, 2008, **128**, 094306.
23 F. Uhl, L. Walewski, H. Forbert and D. Marx, *J. Chem. Phys.*, 2014, **141**, 104110.
24 H. Schmiedt, P. Jensen and S. Schlemmer, *Phys. Rev. Lett.*, 2016, **117**, 223002.
25 H. Schmiedt, P. Jensen and S. Schlemmer, *Chem. Phys. Lett.*, 2017, **672**, 34–46.
26 H. Schmiedt, P. Jensen and S. Schlemmer, *J. Mol. Spectrosc.*, 2017, **342**, 132–137.
27 J. I. Rawlinson, *J. Chem. Phys.*, 2019, **151**, 164303.
28 L. Pauling, *J. Chem. Phys.*, 1936, **4**, 673–677.
29 J. I. Rawlinson, *Nucl. Phys. A*, 2018, **975**, 122–135.
30 J. I. Rawlinson, PhD thesis, University of Cambridge, 2020.
31 G. Berkolaiko and P. Kuchment, *Introduction to Quantum Graphs*, American Mathematical Society, 2013, vol. 186.
32 P. R. Bunker and P. Jensen, *Molecular symmetry and spectroscopy*, NRC Research Press, Ottawa, 2006.
33 P. R. Schreiner, S.-J. Kim, H. F. Schaefer III and P. von Ragué Schleyer, *J. Chem. Phys.*, 1993, **99**, 3716–3720.
34 A. Witt, S. D. Ivanov and D. Marx, *Phys. Rev. Lett.*, 2013, **110**, 083003.
35 N. Biggs, *Algebraic Graph Theory*, Cambridge University Press, 1993.
36 P. Árendás, T. Furtenbacher and A. G. Császár, *J. Math. Chem.*, 2016, **54**, 806–822.